Data Augmentation for Depression Detection Using Skeleton-Based Gait Information

Jingjing Yang[1,*] , Haifeng Lu[1,*] , Chengming Li[2,†], Xiping Hu[1,2,†] , Bin Hu[1,3,†]

1.School of information Science and Engineering, Lanzhou University, Lanzhou China.

2.Shenzhen Institutes of Advanced Technology, Chinese Academy of Sciences, Shenzhen, China.

3.Institute of Engineering Medicine, Beijing Institute of Technology, Beijing, China.

$\{yangjj19, luhf18, huxp, bh\}@lzu.edu.cn, cm.li@siat.ac.cn$

***Abstract*—In recent years, the incidence of depression is rising rapidly worldwide, but large-scale depression screening is still challenging. Gait analysis provides a non-contact, low-cost, and efficient early screening method for depression. However, the early screening of depression based on gait analysis lacks sufficient effective sample data. In this paper, we propose a skeleton data augmentation method for assessing the risk of depression. First, we propose five techniques to augment skeleton data and apply them to depression and emotion datasets. Then, we divide augmentation methods into two types (non-noise augmentation and noise augmentation) based on the mutual information and the classification accuracy. Finally, we explore which augmentation strategies can capture the characteristics of human skeleton data more effectively. Experimental results show that the augmented training data set that retains more of the raw skeleton data properties determines the performance of the detection model. Specifically, rotation augmentation and channel mask augmentation make the depression detection accuracy reach 92.15% and 91.34%, respectively.**

***Index Terms*—Depression recognition, Kinect, Gait, Data augmentation.**

I. INTRODUCTION

According to the data from the World Health Organization (WHO), there are more than 340 million people worldwide suffering from depression, which has become the second cause of death after cancer [1]. In 2020, the Chinese government proposed mental health services for high-risk crowds, such as teenagers, pregnant women, the elderly, especially depression screening was included in student's physical examination [2]. However, due to the shortage of professional psychiatric doctors and social discrimination associated with mental disorders, large-scale screening for depression is still a challenge. Fortunately, Artificial Intelligence (AI) has made it possible for large-scale depression screening [3], [4], [5].

Some scholars pointed out that there is convincing evidence of bidirectional interactions between depression and gait information [6]. Hence, some scholars pay attention to automatic depression detection using gait analysis integrated with AI technologies [7], [8], [9]. However, there is a common problem that lack sufficient labeled datasets. This problem is affected by objective factors (time, cost), and is difficult to solve in a short time. According to relevant papers, small sample datasets are more likely to overfit during training [10].

† These authors are corresponding author.

∗ These authors have contributed equally to this work.

Therefore, we need to consider how to avoid overfitting in the limited data and improve the performance of the depression detection model as far as possible.

Data augmentation includes a set of techniques that can augment the size and quality of training datasets, and it has been proved to be effective to improve the performance of the deep learning models [11]. Data augmentation methods can obtain a more complex representation of the raw data, reduce the gap between the training set and test set, and enable the neural network to better understand the distribution of data on the dataset. Existing data augmentation technologies are divided into two aspects: data warping and oversampling [12]. Data warping augmentations convert existing images, including geometric and color transformations, random erasing, adversarial training, and neural style transfer. Oversampling augmentations create synthetic instances and add them to the training set, including mixing images, feature space augmentations, and the Generative Adversarial Networks (GAN) [13].

Differential data augmentation techniques have been proposed in computer vision, including Random Erasing [14], AutoAugment [15], GridMask [16]. Although different augmentation strategies and their combinations have been investigated widely for image recognition tasks, the augmentation strategies for skeleton-based gait data are rarely studied. The lack of gait training data makes it critical to explore data augmentation strategies.

In this work, we preprocess the skeleton-based gait data collected by the Kinect camera firstly. Then, we propose five augmentation methods for skeleton-based gait data. Thirdly, we apply five augmentation methods to the postgraduate depression gait dataset and use two deep learning models (Longterm Short-Term Memory (LSTM) [17] and Temporal Convolutional Network (TCN) [18]) to test our method. Finally, we verify the experimental results on the public emotion dataset and analyze the augmentation effects of these methods based on the mutual information between the augmented data and the raw data. The results show that the augmentation methods can be divided into two types: non-noise augmentation and noise augmentation. The effect of non-noise augmentation is obviously better than that of noise augmentation. Rotation and channel mask augmentations increase the classification accuracies to 92.15% and 91.34% respectively.

In summary, we make the following contributions:

• In order to solve the problem of insufficient sample

gait data, five data augmentation methods (rotation, shear, Gaussian noise, channel mask, and joint mask) are proposed. Experimental results show that the augmentation strategy has a significant impact on the depression detection models, the rotation and channel strategies increase the accuracy by about 6%.

- By calculating the mutual information between the augmented data and the raw data, the proposed augmentation methods on skeleton-based gait data are divided into two types: non-noise augmentation and noise augmentation. These two types can preliminary estimate the results of data augmentation.

- We analyze the impact of five data augmentation methods on classification accuracy and conclude that augmented training data set that retains properties more of the raw skeleton data properties determines the performance of the model. This provides an idea for the application of data augmentation for depression detection using gait analysis in the future.

The rest of this paper is organized as follows: Sec. II introduces the research status of depression recognition and the background of data augmentation. Two gait datasets and five proposed data augmentation methods are depicted in Sec. III. Sec. IV presents the experimental results and gives a comprehensive discussion of the proposed methods combined with the mutual information. The conclusion of this paper described in Sec. V.

II. RELATED WORK

A. Depression recognition and gait

At present, the clinical diagnosis of depression is mainly based on symptoms, mental and scale examinations by psychiatrists [19]. However, most depression patients do not ask for help in time because patients usually cannot realize that they have depression in the early stages of depression. In recent years, many scholars recognize depression from the perspective of facial expression, voice, physiological signal, video, *etc.* [20], [21], [22]. However, the detection of physiological signals requires a accurate detection system in a restrictive environment; Facial expression and voice collection need emotional stimulation in a specific environment. Therefore,large-scale depression detecting is still a difficult problem.

Research shows that emotion is interlocked with perception, cognition, motivation, and action [23]. Many scholars have studied the relationship between gait and emotion, e.g., happy walkers display an increase in gait speed, step length, arm swing, *etc.*; Sad walkers display a decrease in gait speed, step length, arm swing, *etc.* [24], [25], [26], [27]. Long-term exposure to negative emotions may lead to changes in brain areas related to perception, cognition, and motor systems [28].

In some studies on the gait of people with depression, the researchers found that depression patients have a reduced gait velocity, vertical head movement, arm swing, stride length, *etc.* [29], [30]. In [31], Wang *et al.* extracted a novel Time-domain and Frequency-domain feature (TF-feature) and a Spatial Geometric feature (SG-feature), and investigated the effectiveness of fused features of gait data for the non-contact depression detection. A rigid-body representation of the human body was proposed in [32], which can improve the robustness of detecting depression patients with noisy input and reduce the classification time.

In previous studies, scholars have been committed to exploring new gait features and using traditional machine learning models for classification, and the accuracy has been continuously improved. However, traditional machine learning technologies were limited in their ability to process natural data in their raw form, and lack the ability to express complex functions, making it difficult to solve more complex natural signal processing problems. Deep learning allows computational models that are composed of multiple processing layers to learn representations of data with multiple levels of abstraction, and demonstrate a powerful ability to learn the essential characteristics of a data set from a small number of samples [33]. At present, few people applies deep learning methods to gait depression recognition.

B. Data augmentation

In [34], the authors pointed out data augmentation can be divided into augmenting raw data and feature space. After experimental comparison, it is found that augment raw data is better. Therefore, we focus on the raw data which is three-dimensional skeleton data collected by Kinect. In this paper, geometric transformation and random erasure are mainly used. Geometric transformation includes three methods: rotation, shearing, and adding Gaussian noise. Random erasure refers to hiding some random or specific point data. Of course, the use of GAN for style transfer and feature space data augmentation is also a problem worthy of further study.

Rotation, noise injection and random erasing are commonly image augmentation methods. Rotation augmentation is accomplished by rotating the image right or left on an axis between $1°$ and $359°$ [10]. Noise injection consists of injecting a matrix of random values usually drawn from a Gaussian distribution [10]. Moreno-Barea *et al.* confirmed that adding noise to the images can help CNN learn more robust features by testing on 9 datasets [35]. Random erasing [36] is a data augmentation technique developed by Zhong *et al.*, which can be understood as losing part of the data information before entering the network. Random erasing forces the model to learn more descriptive features about the rest of the image, thereby preventing the model from overfitting certain visual features of the image. In this paper, we use two random erasing strategies: joint mask and channel mask.

Variational auto-encoders (VAE) [37] have become a popular method of unsupervised learning. They are constructed by neural networks and can be trained with stochastic gradient descent [38]. VAE has shown good prospects for generating complex data including handwritten digits, faces, physical models of house numbers, segmentation, and predicting the future from static images.

GAN architecture proposed by Ian Goodfellow firstly [13] is a framework for generative model through adversarial training. GAN architecture is composed of a generative model and a discriminative model that antagonize each other. In the most ideal state, the generator can generate images that are difficult

for the discriminator network to judge "real and false". The excellent performance of GAN has made people pay more and more attention to how to apply it to data augmentation. [39], [40], [41].

III. METHOD

A. Dateset

1) Depression dataset: In this paper, we use the skeleton coordinate data of 95 postgraduate students aged 22 to 18 [32], including 43 scored-depressed students and 52 non-depressed students based on the scores of the Patient Health Questionnaire (PHQ-9, Chinese version) [42] and Zung Self-rating Depression Scale (SDS, Chinese version) [43]. All participants were asked to walk forth and back twice on a 10-meter-long path at a comfortable speed and posture. Two Microsoft Kinect V2 cameras were used to obtain data of 25 joint points (as shown in Fig. 1) of the human body.
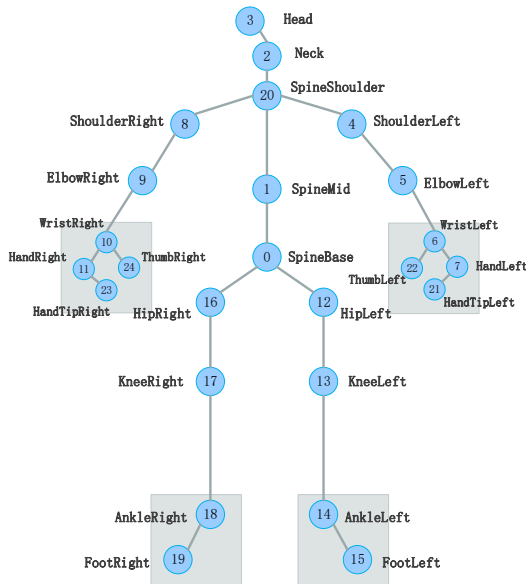

Fig. 1. The diagram of joints location [44].

2) Emotion dataset:

We use the part of the emotional multimodal database that records the skeletal points of the human body [45]. During the collection process, all actors were required to perform emotional states separately in the following order: neutral, sadness, surprise, fear, disgust, anger, and happiness. Without any guidance or prompts from the researcher, everyone performed each emotion five times. The Kinect V2 sensor was used to capture the skeleton data of 25 joint points of the human body. Except for some poor quality data, the emotional skeleton database used in this study finally contains 474 samples of 13 participants.

B. Data preprocessing method

1) Depression dataset:

The preprocess of the depression dataset includes the following four processes: data filtering, angle transformation, denoise and re-sampling, and data simplification.

Data Filtering: During the collection, the device estimated the coordinates of the skeleton joints from the front view and the back view. In the first step, we segment them into two streams of data. According to previous reports, the estimated skeleton in the back view is not as accurate as the skeleton in the front view. Therefore, we only analyze the skeleton in the front view. The second step is to observe whether the target skeleton presents a good shape and delete the data of limbs deformation.

Angle Transformation: Because the camera has an angle to the ground, participants do not walk horizontally along the Z axis in the Kinect coordinate system. System errors are introduced when filtering Z-axis data. In order to analyze the data accurately, the coordinate system of the raw data must be converted. We perform coordinate transformation on all recorded data according to the transformation matrix in Eq. 1.

$$\begin{bmatrix} x' \ y' \ z' \end{bmatrix} = \begin{bmatrix} x \ y \ z \end{bmatrix} \begin{bmatrix} 1 & 0 & 0 \\ 0 & \cos\theta & \sin\theta \\ 0 & -\sin\theta & \cos\theta \end{bmatrix} \quad (1)$$

where $[x'\ y'\ z']$ is the joint position after coordinate transformation; $[x\ y\ z]$ is the raw data; θ is the angle between the Kinect camera and the ground, calculated by the formula in [32].

In the Kinect coordinate system, each participant's walking trajectory is different. In order to eliminate the influence of absolute position information, the skeleton coordinates must be projected from the sensor space to the local space of the human body, and the center of the local space is located on the SpineBase joint (joint 0 in Fig. 1). The formula is shown in Eq. 2. As a result, vectors containing the position and direction of each joint relative to the Spinebase joint are obtained.

$$norm\_joint = joint - spinebase \quad (2)$$

De-noise and Re-sampling: The Kinect camera is affected by different factors such as light and colors of the subject's clothes, which generate noise in the collected data. We use Gaussian filter [46] to smooth data, reduce high-frequency noise, and increase identifiability [7], [8]. The length of the Gaussian filter window is 5, and the convolution kernel is $1/16 \times [1,4,6,4,1]$. It filters the x-axis, y-axis and z-axis data separately based on the timestamp.

Data Simplification: During the process of data collection, participant's hand joints are prone to misidentification and there is almost no movement among the fingers when walking [45]. In order to reduce the impact of error data on the training model, the average value of the left hand (joints $6, 7, 21, 22$ in Fig. 1) or the right hand (joints $10, 11, 23, 24$ in Fig. 1) is taken as the human hand coordinate. In addition, since the Kinect hanging on the ceiling will cause distortion of the recognition of the joints of the foot, we take the average value instead of them respectively. After data simplifying, the number of skeleton joints is changed from 25 to 17. This part

is only suitable for rotation, adding Gaussian noise and shear augmentations.

2) Emotion dataset:

Firstly, similar to the coordinate transformation method mentioned above, raw Kinect V2 data is affected by the distance between the actor/actress and the sensor during recording. Skeleton coordinates must be projected from the sensor space to the local space of the human body. Secondly, in order to unify the joint position values between higher and lower individuals, we use normalisation based on the distance between two joints with the lowest position noise in all records: SpineBase (joint 0 in Fig. 1) and SpineShoulder (joint 20 in Fig. 1). The normalization process follows Eq. 3.

$$d_i = \frac{J_i}{J_{20} - J_0},$$ (3)

where d_i is the distance vector between the i and J_0 joints. $J_{20} - J_0$ refers to the difference between the individual joints J_{20} (SpineShoulder) and J_0 (SpineBase) in the neutral state. J_i refers to the joint vector of each joint point in the seven emotional states.

C. Rotation and translation

Through the conversion of the original data, we obtain the skeleton data under different virtual cameras. The schematic is shown in Fig. 2, where the black dots are the locations of the virtual camera in different views. The specific operation steps are as follows. We take the participant as the center, and suppose the camera rotates and translates around the participant. The rotation angle refers to the position of cameras in Chinese Academy of Sciences Institute of Automation (CASIA) dataset [47], increasing by $18°$ each time.
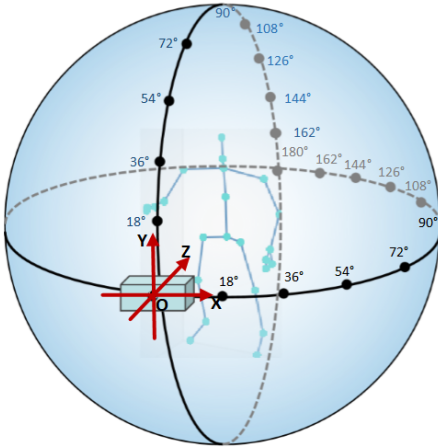

Fig. 2. The schematic of rotation augmentation.

We rotate the camera to the same angle with CASIA dataset. According to Eq. 4, the camera is rotated horizontally to the position of '$X_\alpha O Z_\alpha$' in Fig. 3. Since the camera revolves horizontally with the participant's SpineBase joint as the center, the change of y-axis is not involved. When rotating in the vertical direction, the *ZOY* plane also performs the same operation without changing the x-axis. The formula is shown in Eq. 5.

$$[\,x_\alpha \; y_\alpha \; z_\alpha\,] = [\,x' \; y' \; z'\,] \begin{bmatrix} \cos\delta & 0 & -\sin\delta \\ 0 & 1 & 0 \\ \sin\delta & 0 & \cos\delta \end{bmatrix}$$ (4)

$$[\,x_\beta \; y_\beta \; z_\beta\,] = [\,x' \; y' \; z'\,] \begin{bmatrix} 1 & 0 & 0 \\ 0 & \cos\delta & \sin\delta \\ 0 & -\sin\delta & \cos\delta \end{bmatrix}$$ (5)

where δ is the rotation angle, $[\,x' \; y' \; z'\,]$ is the origin coordinate; $[\,x_\alpha \; y_\alpha \; z_\alpha\,]$ and $[\,x_\beta \; y_\beta \; z_\beta\,]$ are the coordinates after horizontal and vertical rotation respectively.
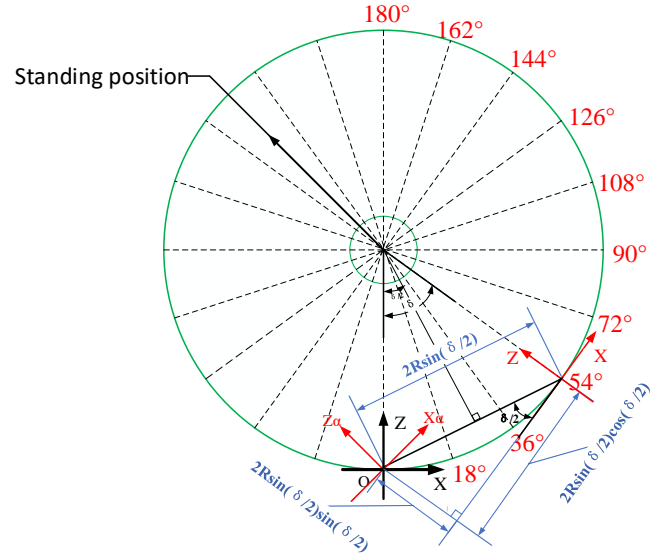

Fig. 3. The planform of camera position rotation.

According to the scenario in Fig. 2, we need to translate the data. First, set the distance between the camera and the human body to 3. Second, the displacement distance of the origin is obtained according to the geometric relationship in 3. The calculation process is shown in Eq. 6 and Eq. 7. For example, when the angle is equal to $54°$, the coordinate system $X_{54} O Z_{54}$ in Fig. 3 is the position *XOZ* after the rotation and translation. Finally, the camera is rotated and translated in the *XOZ* plane and the *YOZ* plane.

$$\begin{cases} x'' = x_\alpha - 2R \sin\left(\frac{\delta}{2}\right) \cos\left(\frac{\delta}{2}\right) \\ y'' = y_\alpha \\ z'' = z_\alpha + 2R \sin\left(\frac{\delta}{2}\right) \sin\left(\frac{\delta}{2}\right) \end{cases}$$ (6)

$$\begin{cases} x'' = x_\beta \\ y'' = y_\beta - 2R \sin\left(\frac{\delta}{2}\right) \cos\left(\frac{\delta}{2}\right) \\ z'' = z_\beta + 2R \sin\left(\frac{\delta}{2}\right) \sin\left(\frac{\delta}{2}\right) \end{cases}$$ (7)

After rotation and translation, we choose different δ to augment the data. The angles of $18°$, $36°$, $54°$, $72°$, $90°$, $108°$, $126°$, $144°$, $162°$, and $180°$ are transformed in horizontal and vertical directions. The visualization pictures are shown in Fig. 4. Fig. 4. a) is the raw data, and Fig. 4. b) - Fig. 4. e) correspond to the transformation results of $36°$, $72°$, $108°$, and $144°$ respectively in the horizontal direction. Fig. 4. f) - Fig. 4. h) correspond to the transformation results of $36°$, $54°$, $108°$, and $144°$ respectively in the vertical direction.

(a) raw   (b) raw-36-h   (c) raw-72-h

(d) raw-108-h   (e) raw-144-h   (f) raw-36-v

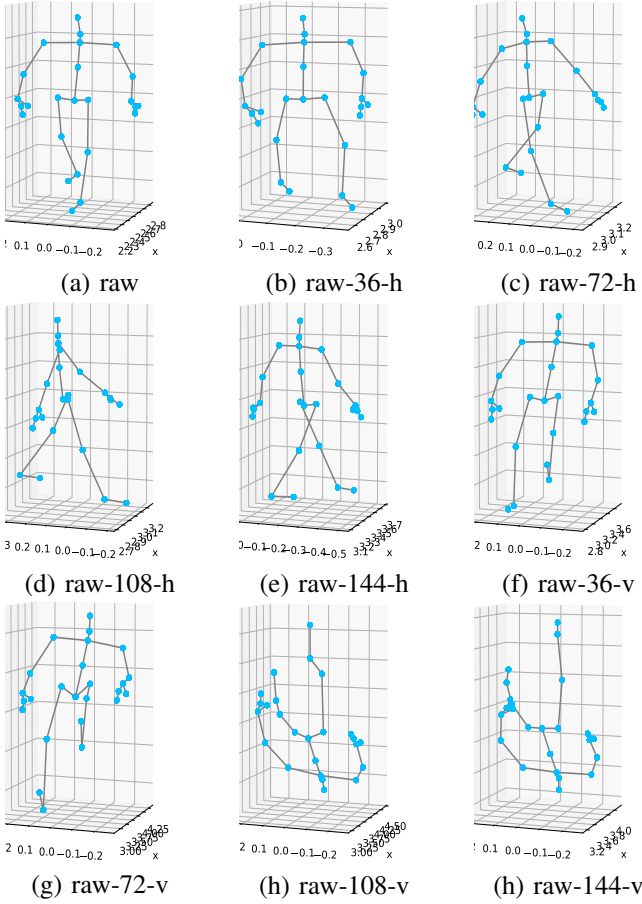(g) raw-72-v   (h) raw-108-v   (h) raw-144-v

Fig. 4. Visualization of rotation augmentation.

D. Shear

The shear transformation simulates the possible morphological changes of the skeleton caused by the system noise during the collection process. It is a linear mapping, and each joint can be moved in a fixed direction. The 3D coordinate shape of human joints can be tilted at any angle. The visualization pictures are shown in the Fig. 5 and shear transformation matrix is defined as:

$$S = \begin{bmatrix} 1 & s_1 & s_2 \\ s_3 & 1 & s_4 \\ s_5 & s_6 & 1 \end{bmatrix} \tag{8}$$

where $s_1, s_2, s_3, s_4, s_5, s_6$ are shear factors sampled randomly from [-1,1]. All joint coordinates of the raw skeleton sequence are transformed by the shear matrix matrices.

E. Gaussian noise

Gaussian noise is an error in accordance with Gaussian normal distribution. In some cases, we need to add appropriate Gaussian noise to the standard data to make the data have certain errors. The visualization pictures are shown in Fig. 6.

F. Joint mask

We employ the zero-mask (i.e., replace all coordinates by zeros) to a number of body joints in skeleton frames,
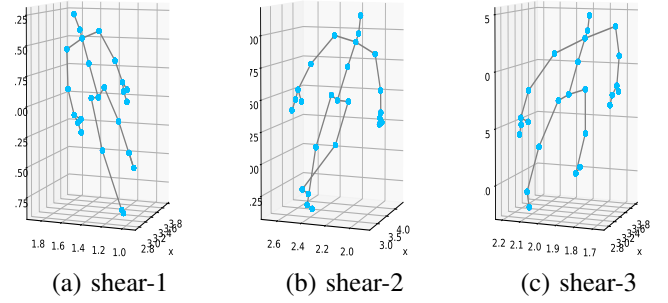

(a) shear-1   (b) shear-2   (c) shear-3

Fig. 5. Visualization of shear augmentation.
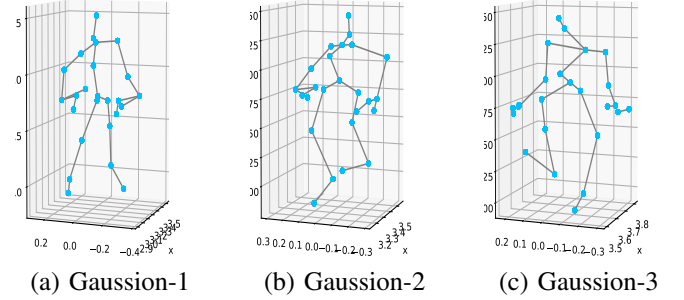

(a) Gaussion-1   (b) Gaussion-2   (c) Gaussion-3

Fig. 6. Visualization of Gaussion noise augmentation.

which extends the pixel-level "Cutout" operation in image augmentation to joint-level skeleton sequences. This method simulates the situation where the body is obscured when collecting data, allowing the model to learn different local regions (except for the masked region) that probably contain crucial action patterns. More specifically, we randomly or specifically select body joints from random frames in the raw skeleton sequence to apply the zero-mask. The visualization pictures are shown in Fig. 7.

(a) joint-1   (b) joint-2   (c) joint-3
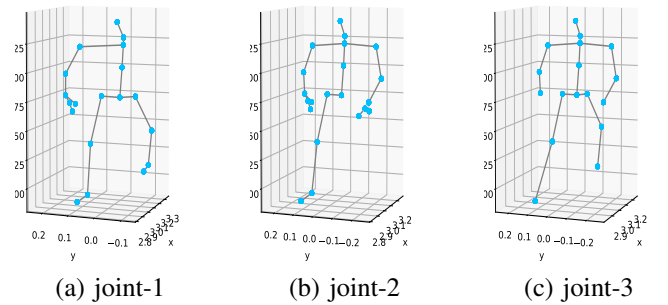
Fig. 7. Visualization of Joint Mask augmentation.

G. Channel mask

The channel mask tries to simulate the skeleton at different viewing angles. We select a "channel" (an axis A $\in$ {X, Y, Z}) of the skeleton sequence separately, and apply the zero mask to all coordinates on this axis. In this way, the raw 3D skeleton sequence can be converted into a projected 2D sequence, so that the model can learn the changes in the human body's movement during walking from a specific two-dimensional plane. The visualization pictures are shown in Fig. 8.

(a) channel-x   (b) channel-y   (c) channel-z

Fig. 8. Visualization of Channel Mask augmentation.

IV. EXPERIMENT RESULTS AND DISCUSSION
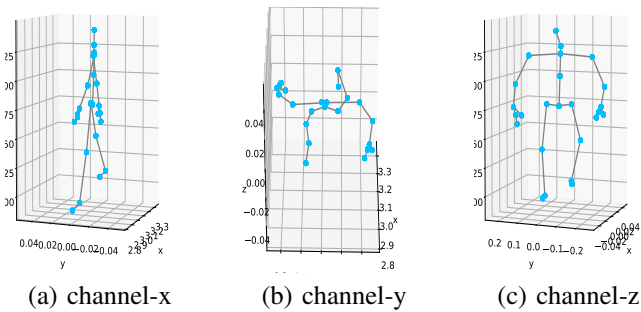
A. Classified method

In this paper, we apply two different deep learning neural networks to the augmented composite dataset to evaluate proposed data qugmentation methods by comparing their performance based on recognition rate. Because of the time series of gait skeleton data, we run two deep learning models (LSTM and TCN) under the framework of tensorflow2.0 in python 3.8. The above classification methods are described below.

LSTM is composed of 7-layer neural networks, including an input layer, two LSTM layers, two Dropout layers, a Flatten layer and a Dense layer. Two LSTM layers have 128 and 512 neurons respectively. In order to avoid overfitting, we set the dropout to 0.2. The activation function is Tanh, and the loss function is the categorical crossentropy. The optimization algorithm of the model uses the Adam algorithm. A total of 200 epochs are trained, where the initial learning rate is 0.01 and batch size is 64.

TCN is composed of nine convolution layers (Convolution kernel = 8), in which the stride of the fourth layer and the seventh layer is 2, and the stride of the remaining layers is 1. Each layer of the 1st-3rd layers has 64 neurons. Each layer of the 4th-6th layers has 128 neurons. Each layer of the 7th-8th layers has 256 neurons. The activation function is Relu and the dropout is 0.1. The optimizer is Adam. The loss function is the categorical cross entropy, and the batch size is 32.

We divided all participants' segments into a training set and a testing set according to the proportion of 4:1. In order to ensure the validity of the experimental results, the fragments are randomly divided by person, that is, fragments of the same person only appear in one group. On this basis, the training set and the test set are expanded to 5:1 and 3:1. Each augmentation method is tested on these three groups.

B. Experimental results of rotation and translation augmentation

According to the rotation strategy proposed in the previous part of this paper, we carried out 11 groups of experiments in the vertical and horizontal directions respectively. Table I and Table II show the classification results. One can see that from the data in Table I and Table II, the classification accuracy after rotation augmentation has been improved in some angles, the highest accuracy up to 92.15% (the data with * in the table indicates that the accuracy after augmenting this angle is

higher than the raw data). When the rotation angle is $18°$ and $36°$, the augmentation effect is significant, and the accuracy is improved in the three test sets. As the rotation angle increases, the difference between the raw data and the augmentation data is too large, so that the network cannot learn useful features.

C. Experimental results of shear augmentation

The shear matrix in Eq. 8 contains six shear factors, all of which are randomly generated from [-1,1]. In this paper, three groups of random shear augmentation experiments are carried out. In each group of experiments, each segment uses a different augmentation factor. From the experimental results in Table III, it can be seen that the classification accuracy is unstable after shear augmentation. The highest accuracy rate is 91.97% and the lowest is 71.53%. In $4:1$ case, the average accuracy of the three groups under the LSTM model is 83.17%, but the accuracy of the third group is 14% higher than that of the second group.

D. Experimental results of channel mask augmentation

We perform four sets of experiments, and the results are shown in the Table IV. We find that after deleting the x-axis data, the classification accuracy is improved by more than 5%, reaching 91.34%; after deleting the z-axis data, it is greatly reduced.

E. Experimental results of adding Gaussian noise

Noise may occur during data collection, transmission or processing, and noise is inevitable. In order to simulate the noise position that may appear in the above process, we add Gaussian noise N(0,0.05) to the joint coordinates of the raw sequence. The experiment results of three groups are shown in Table V. After the first group of Gaussian augmentation, the accuracy of the two models increase to more than 90%, up to 93.43%, while the third group decreased significantly. The difference in classification accuracy between the two groups is more than 20%, indicating that the result of adding Gaussian noise is unstable.

F. Experimental results of joint mask augmentation

We explored the effects of removing the joints of the limbs, torso, upper body, and lower body on the recognition of depression. The classification results are shown in Table VI. After removing any group of data from the limbs, trunk, upper body and lower body, the accuracy decrease, indicating that the gait features of any part cannot be ignored. Then, add four groups of random trials and randomly delete the key nodes of 20%, 40%, 60%, 80%. After deleting too many joint points, the accuracy is greatly reduced.

G. Discussion

The above experiments prove that proposed augmentation strategies have a significant impact on the classification results. In order to analyze the reasons for the differences in classification accuracy of different strategies, we calculate the

TABLE I
CLASSIFICATION RESULTS OF DIFFERENT ROTATION ANGLES IN THE HORIZONTAL DIRECTION

		raw	raw+18	raw+36	raw+54	raw+72	raw+90	raw+108	raw+126	raw+144	raw+162	raw+180
3:1	LSTM	0.8431	**0.8996***	0.8850*	0.8442*	0.8326	0.8576*	0.8412	0.8631*	0.8667*	0.8759*	0.84125
	TCN	0.8686	**0.9197***	0.9051*	0.8099	0.8017	0.7973	0.8262	0.7973	0.8079	0.8332	0.8557
4:1	LSTM	0.7919	**0.8101***	0.8081*	0.7516	0.7452	0.7635	0.7896	0.8209*	0.8205*	0.8124*	0.7694
	TCN	0.7919	**0.8751***	0.8334*	0.7921	0.7914	0.8358*	0.8138*	0.7715	0.7961*	0.7921	0.8123*
5:1	lSTM	0.8430	**0.8978***	0.8579*	0.8065	0.8045	0.8073	0.8394	0.8502*	0.8047	0.8175	0.8467*
	TCN	0.8540	**0.8923***	0.8226	0.8089	0.8061	0.8010	0.8116	0.7700	0.7835	0.8357	0.8593*

TABLE II
CLASSIFICATION RESULTS OF DIFFERENT ROTATION ANGLES IN THE VERTICAL DIRECTION

		raw	raw+18	raw+36	raw+54	raw+72	raw+90	raw+108	raw+126	raw+144	raw+162	raw+180
3:1	LSTM	0.8431	**0.9051***	0.8988*	0.8649*	0.8428	0.8558*	0.8485*	0.8540*	0.8631*	0.8503*	0.8923*
	TCN	0.8686	**0.9215***	0.8832*	0.8047	0.8034	0.8083	0.8007	0.7937	0.8057	0.7956	0.8833*
4:1	LSTM	0.7919	**0.8486***	0.8065*	0.8125*	0.7866	0.7682	0.8285*	0.8446*	0.8056*	0.8183*	0.7682
	TCN	0.7919	0.8445*	**0.8478***	0.8147*	0.8279*	0.8467*	0.8547*	0.7810	0.7925*	0.7859	0.8302*
5:1	lSTM	0.8430	**0.8759***	0.8448*	0.8357	0.8314	0.8503*	0.8510*	0.8248	0.8284	0.8266	0.8029
	TCN	0.8540	0.8649*	**0.9069***	0.8305	0.8291	0.8175	0.8098	0.8503	0.7953	0.8489	0.8043

TABLE III
CLASSIFICATION RESULTS OF SHEAR AUGMENTATION

		raw	1	2	3
3:1	LSTM	0.8430	0.8511	0.8105	0.9197
	TCN	0.8686	0.8777	0.8323	0.7943
4:1	LSTM	0.7919	0.8029	0.7726	0.9197
	TCN	0.7919	0.7992	0.8686	0.7153
5:1	LSTM	0.8430	0.8868	0.8014	0.8120
	TCN	0.8540	0.8333	0.8467	0.7888

TABLE IV
CLASSIFICATION RESULTS OF CHANNEL MASK AUGMENTATION

		raw	raw+subx	raw+xuby	raw+subz
3:1	LSTM	0.8430	**0.9035**	0.8553	0.7689
	TCN	0.8686	**0.9134**	0.8448	0.6587
4:1	LSTM	0.7919	**0.8662**	0.8196	0.6886
	TCN	0.7919	**0.8705**	0.7973	0.6329
5:1	LSTM	0.8430	**0.8981**	0.8571	0.7379
	TCN	0.8540	**0.9095**	0.8540	0.6313

TABLE V
CLASSIFICATION RESULTS OF GAUSSIAN AUGMENTATION

		raw	1	2	3
3:1	LSTM	0.8430	0.9087	0.9288	0.7197
	TCN	0.8686	0.9243	0.8099	0.7434
4:1	LSTM	0.7919	0.9343	0.9032	0.7281
	TCN	0.7919	0.9343	0.7921	0.7921
5:1	LSTM	0.8430	0.9324	0.9069	0.7527
	TCN	0.8540	0.9107	0.7989	0.7914

mutual information (MI) between the augmented data and the raw data. MI is an indicator to measure the "similarity" and it provides a general measure of dependence between variables [48]. The calculation formula of mutual information is Eq. 11, which is derived from Eq. 9-10. Eq. 9 defines entropy, which is the average amount of information contained in each received message. The joint entropy H(A, B) of two discrete systems A and B is defined analogously in Eq. 10.

$$H(A) = -\sum_{j=1}^{M_A} p(a_j) \log p(a_j) \tag{9}$$

$$H(A, B) = -\sum_{a,b} P_{AB}(a, b) \log P_{AB}(a, b) \tag{10}$$

$$I(A, B) = H(A) + H(B) - H(A, B) \tag{11}$$

Table VII shows the average mutual information between each augmented dataset and the raw dataset. It can be seen from the table that the average mutual information of data augmented by rotation and channal mask is larger, while it of the data augmented by the other three augmentation methods is relatively small. Combined with the principle of data augmentation, the data augmentation methods mentioned in this article can be divided into two categories. One is non-noise augmentation, that is, the basic shape of the skeleton is maintained during the data augmentation process, and the basic gait information is still retained. Such methods are mainly rotation and channel mask. The other is noise augmentation, that is, the skeleton structure changes in the process of data augmentation, leading to the deformation of the body. Such methods are mainly shearing and adding Gaussion noise.

From the data in Table I- Table V, it can be observed that the effect of non-noise augmentation is significantly better than that of noise augmentation. For example, when rotating the smaller angles of 18° and 36°, experimental results of both horizontal and vertical are significantly improved in the

TABLE VI
CLASSIFICATION RESULTS OF JOINT MASK AUGMENTATION

		raw	raw+Upper_body	raw+Lower_body	raw+Trunk	raw+Limbs	1	2	3	4
3:1	LSTM	0.8430	0.7923	0.8032	0.8288	0.7686	0.7916	0.9178	0.8087	0.7596
	TCN	0.8686	0.7589	0.7975	0.7501	0.6812	0.7912	0.7828	0.85558	0.6624
4:1	LSTM	0.7919	0.7798	0.7080	0.7244	0.7116	0.8014	0.7812	0.6916	0.7135
	TCN	0.7919	0.6770	0.7224	0.7088	0.6569	0.7708	0.8083	0.8188	0.8211
5:1	LSTM	0.8430	0.7651	0.7996	0.7406	0.8321	0.8080	0.9251	0.8130	0.7211
	TCN	0.8540	0.7408	0.7927	0.6770	0.6441	0.7656	0.8010	0.8615	0.6694

TABLE VII
AVERAGE MUTUAL INFORMATION OF DIFFERENT AUGMENTATION
METHODS IN DEPRESSION DATA

Rotation	Channel Mask	Gaussion Noise	Shear	Joint Mask
6.4364	6.4207	5.1456	5.1438	4.9169

three groups of ratios. When the vertical rotation is 36°, the highest accuracy is 92%, and the accuracy of other angles is improved by at least 2%. As the angle increase, the difference between the raw data and the augmented data becomes larger and the classification accuracy shows a downward trend. In all 6 groups of results for deleting the x-axis, the accuracy of the channel mask is improved by at least 5%. These two augmentation methods are non-noise augmentation, and both maintain the basic shape of the skeleton and the raw gait information. However, because the augmentation process of shearing and adding Gaussian noise is random, the structure of the skeleton changes after the augmentation and the classification effect is unstable.

According to [49], adding appropriate data noise can improve the stability of the network and reduce the overfitting of training, but too much noise will mask the raw information of the data, thus reducing the accuracy of the model. Rotation augmentation and channel mask augmentation add appropriate noise to the raw data to improve the robustness of the model, while shear and Gaussian noise add too much noise, resulting in the network to learn a lot of biased data information in the training process.

In order to verify the above conclusions, we did the same experiment using the LSTM model on the emotion dataset mentioned above, and randomly selected 70 fragments of 2 participants as the test set and the other 11 participants as the training set. The mutual information and LSTM classification accuracies between each augmented dataset and raw dataset in the rotation augmentation are given in Fig. 9 and Fig. 10. When rotating at a small angle in the vertical and horizontal directions, they all have higher mutual information and higher classification accuracy. The results of other augmentation methods are shown in the Table VIII. After deleting the x-axis data in channel mask augmentation, the accuracy of the model is improved; After deleting the z-axis, the accuracy is still lower than the raw data, and the corresponding mutual information of the data after deleting the x-axis is greater than the data after deleting the z-axis. Random experiments are carried out for three augmentation methods: shear, Gaussian

noise and joint mask. Similar to the depression data, the experimental results in each group are not stable.
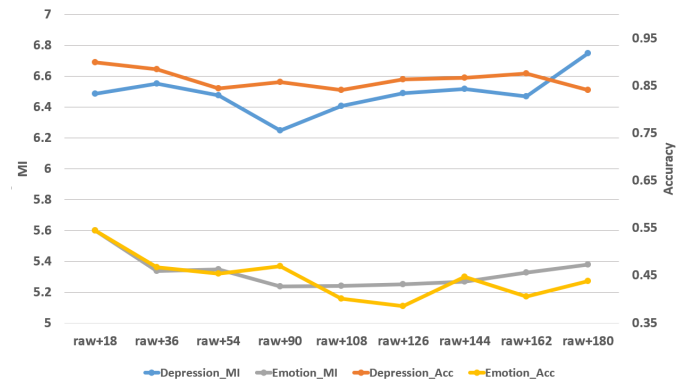

Fig. 9. Comparison chart of rotation augmentation and accuracy in the horizontal direction
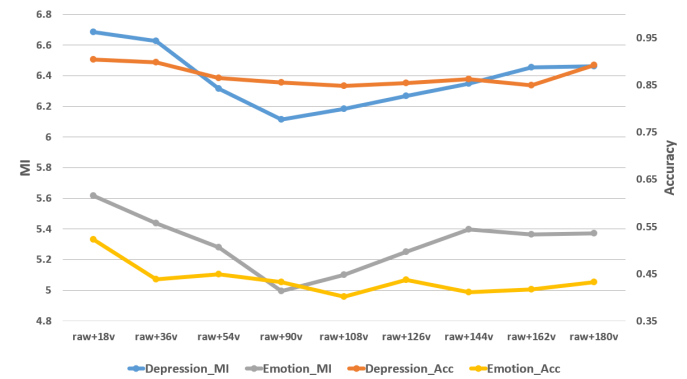

Fig. 10. Comparison chart of rotation augmentation and accuracy in the vertical direction

These values enable us to explore the relationship between the mutual information of gait skeleton information generated from an augmentation strategy and the test accuracy of LSTM trained on that augmented training set. In other words, we attempt to determine if the extent to which an augmentation captures information about the raw training set affects the classification accuracies. Looking at the results in the figure, we notice that when using the non-noise augmentation methods, higher mutual information is correlated with higher classification accuracy. Specifically, the augmentations that result in data have mutual information of approximately $6.3 - 6.4$ (rotation, channel mask) have accuracies of around

TABLE VIII
ACCURACY AND MUTUAL INFORMATION RESULTS OF DIFFERENT AUGMENTATION METHODS

		Raw	Channel Mask			Gaussion Noise			Shear			Joint Mask			
			raw+subx	raw+suby	raw+subz	1	2	3	1	2	3	1	2	3	4
Depression	MI	-	6.5910	6.5113	6.1598	5.3136	5.0620	5.0612	5.2258	5.1094	5.0960	6.1348	6.1075	5.1751	4.2244
Data	ACC	0.7919	0.8662	0.8196	0.6886	0.9343	0.9032	0.7281	0.8029	0.7726	0.9197	0.7814	0.7812	0.6916	0.7135
Emotion	MI	-	4.218	4.0167	3.2506	3.9731	2.9616	3.9738	3.1721	3.5317	3.1372	3.3829	4.1910	2.7314	2.9880
Data	ACC	0.4188	0.6667	0.5833	0.3846	0.6875	0.3646	0.5677	0.4948	0.5365	0.3750	0.4844	0.7945	0.3802	0.3437

0.8 and the accuracy varies with the rise and fall of the mutual information. While the accuracy of the augmentation data (shear, Gaussian noise) with an average mutual information of about 5.1 is quite unstable.

Combining the above analysis, our conclusion is the augmented training data set that retains more of the raw skeleton data properties determines the performance of the detection model. Small angle rotation and x-axis have a large amount of mutual information between the augmented data and the raw data, indicating that it greatly retains the raw skeleton information, and the corresponding classification accuracy is higher. However, shear, Gaussian noise and joint mask augmentation have little mutual information between the augmented data and the raw data. These augmentation methods deform the raw skeleton, which adds more noise to the training data and seriously affects the accuracy of classification.

Generally, this paper proposes five depression data augmentation methods and explores the effectiveness of these five methods in combination with mutual information. Compared with previous studies, this is the first time that the data augmentation method has been applied to the gait dataset. It solves the problem that the scene is difficult to cover in the process of gait data collection, the collection angle is single, and the neural network is easy to overfit. However, the following problems also existed in the research process. First of all, only the five augmentation methods are discussed separately, and there is no further discussion on the combination method. Second, accuracy. At present, the best result of this paper can reach 92.15%, which is far from the actual application and needs to be further improved.

V. CONCLUSIONS AND FUTURE WORK

In this paper, we propose five methods to augment depression skeleton data, and further explore the effectiveness of those. By comparing the classification results of the two datasets and the mutual information between the augmented data and the raw data, the augmentation methods are divided into non-noise augmentation and noise augmentation, and the effect of non-noise augmentation is obviously better than noise augmentation. Then, combined with the principles of various augmentation methods, we conclude that the augmented training data set that retains more of the raw skeleton data properties determines the performance of the detection model.

In future work, we will continue to explore other augmentation strategies and combine neural networks to achieve faster and more accurate depression recognition. At the same time, we will further study the relationship between gait and depression, and explore more efficient and more suitable depression screening methods.

REFERENCES

[1] World health organization. https://www.who.int/news-room/fact-sheets/detail/depression. accessed on 11 Auegst 2020.

[2] National health commission. http://www.chinanews.com. accessed on 17 September 2020.

[3] LD Branco, C Cotrena, A Ponsoni, R Salvador-Silva, SJL Vasconcellos, and RP Fonseca. Identification and perceived intensity of facial expressions of emotion in bipolar disorder and major depression. *Archives of Clinical Neuropsychology*, 33(4):491–501, 2018.

[4] Jeffrey F Cohn, Nicholas Cummins, Julien Epps, Roland Goecke, Jyoti Joshi, and Stefan Scherer. Multimodal assessment of depression from behavioral signals. In *The Handbook of Multimodal-Multisensor Interfaces: Signal Processing, Architectures, and Detection of Emotion and Cognition-Volume 2*, pages 375–417. 2018.

[5] Fabien Ringeval, Björn Schuller, Michel Valstar, Nicholas Cummins, Roddy Cowie, Leili Tavabi, Maximilian Schmitt, Sina Alisamir, Shahin Amiriparian, Eva-Maria Messner, et al. Avec 2019 workshop and challenge: state-of-mind, detecting depression with ai, and cross-cultural affect recognition. In *Proceedings of the 9th International on Audio/Visual Emotion Challenge and Workshop*, pages 3–12, 2019.

[6] Richard D Sanders and Paulette Marie Gillig. Gait and its assessment in psychiatry. *Psychiatry (Edgmont)*, 7(7):38, 2010.

[7] Jing Fang, Tao Wang, Cancheng Li, Xiping Hu, Edith Ngai, Boon-Chong Seet, Jun Cheng, Yi Guo, and Xin Jiang. Depression prevalence in postgraduate students and its association with gait abnormality. *IEEE Access*, 7:174425–174437, 2019.

[8] Nan Zhao, Zhan Zhang, Yameng Wang, Jingying Wang, Baobin Li, Tingshao Zhu, and Yuanyuan Xiang. See your mental state from your walk: Recognizing anxiety and depression through kinect-recorded gait data. *PLoS one*, 14(5):e0216591, 2019.

[9] YaHui Yuan, Baobin Li, Ning Wang, Qing Ye, Yan Liu, and Tingshao Zhu. Depression identification from gait spectrum features based on hilbert-huang transform. In *International Conference on Human Centered Computing*, pages 503–515. Springer, 2018.

[10] Connor Shorten and Taghi M Khoshgoftaar. A survey on image data augmentation for deep learning. *Journal of Big Data*, 6(1):1–48, 2019.

[11] Zeshan Hussain, Francisco Gimenez, Darvin Yi, and Daniel Rubin. Differential data augmentation techniques for medical imaging classification tasks. In *AMIA Annual Symposium Proceedings*, volume 2017, page 979. American Medical Informatics Association, 2017.

[12] Connor Shorten and Taghi M. Khoshgoftaar. A survey on image data augmentation for deep learning. *Journal of Big Data*, 6(1):1–48, 2019.

[13] Ian Goodfellow, Jean Pouget-Abadie, Mehdi Mirza, Bing Xu, David Warde-Farley, Sherjil Ozair, Aaron Courville, and Yoshua Bengio. Generative adversarial nets. In *Advances in neural information processing systems*, pages 2672–2680, 2014.

[14] Zhun Zhong, Liang Zheng, Guoliang Kang, Shaozi Li, and Yi Yang. Random erasing data augmentation, 2017.

[15] Ekin D. Cubuk, Barret Zoph, Dandelion Mane, Vijay Vasudevan, and Quoc V. Le. Autoaugment: Learning augmentation policies from data, 2018.

[16] Pengguang Chen, Shu Liu, Hengshuang Zhao, and Jiaya Jia. Gridmask data augmentation, 2020.

[17] Sepp Hochreiter and Jürgen Schmidhuber. Long short-term memory. *Neural computation*, 9(8):1735–1780, 1997.

[18] Colin Lea, Rene Vidal, Austin Reiter, and Gregory D Hager. Temporal convolutional networks: A unified approach to action segmentation. In *European Conference on Computer Vision*, pages 47–54. Springer, 2016.

[19] Aaron T Beck and Brad A Alford. *Depression: Causes and treatment*. University of Pennsylvania Press, 2009.

[20] Xiuzhuang Zhou, Kai Jin, Yuanyuan Shang, and Guodong Guo. Visually interpretable representation learning for depression recognition from facial images. *IEEE Transactions on Affective Computing*, 11(3):542–552, 2018.

[21] Jinming Li, Xiaoyan Fu, Zhuhong Shao, and Yuanyuan Shang. Improvement on speech depression recognition based on deep networks. In *2018 Chinese Automation Congress (CAC)*, pages 2705–2709. IEEE, 2018.

[22] Jian Shen, Xiaowei Zhang, Xiao Huang, Manxi Wu, Jin Gao, Dawei Lu, Zhijie Ding, and Bin Hu. An optimal channel selection for eeg-based depression detection via kernel-target alignment. *IEEE Journal of Biomedical and Health Informatics*, 2020.

[23] Pessoa and Luiz. A network model of the emotional brain. *Trends in Cognitive Sciences*, 21(5):357, 2017.

[24] M. Melissa Gross, Elizabeth A. Crane, and Barbara L. Fredrickson. Effort-shape and kinematic assessment of bodily expression of emotion during gait. *Human Movement Science*, 31(1):202–221, 2012.

[25] Gu Eon Kang and M. Melissa Gross. The effect of emotion on movement smoothness during gait in healthy young adults. *Journal of Biomechanics*, page S0021929016311459, 2016.

[26] Johannes Michalak, Nikolaus F. Troje, Julia Fischer, Patrick Vollmar, Thomas Heidenreich, and Dietmar Schulte. Embodiment of sadness and depression–gait patterns associated with dysphoric mood. *Psychosomatic Medicine*, 71(5):580–587, 2009.

[27] Elizabeth Crane and Melissa Gross. Motion capture and emotion: Affect detection in whole body movement. In Ana C. R. Paiva, Rui Prada, and Rosalind W. Picard, editors, *Affective Computing and Intelligent Interaction*, pages 95–101, Berlin, Heidelberg, 2007. Springer Berlin Heidelberg.

[28] Jakob Korf. Qualia in a contemporary neurobiological perspective. *Dialogues in Philosophy Mental & Neuro Sciences*, 2015.

[29] Matthias R Lemke, Thomas Wendorff, Brigitt Mieth, Katharina Buhl, and Martin Linnemann. Spatiotemporal gait patterns during over ground locomotion in major depression compared with healthy controls. *Journal of psychiatric research*, 34(4-5):277–283, 2000.

[30] Joost B Sanders, Marijke A Bremmer, Hannie C Comijs, Dorly JH Deeg, and Aartjan TF Beekman. Gait speed and the natural course of depressive symptoms in late life; an independent association with chronicity? *Journal of the American Medical Directors Association*, 17(4):331–335, 2016.

[31] Tao Wang, Cancheng Li, Chunyun Wu, Chengjian Zhao, Jieqiong Sun, Hong Peng, Xiping Hu, and Bin Hu. A gait assessment framework for depression detection using kinect sensors. *IEEE Sensors Journal*, 21(3):3260–3270, 2020.

[32] Haifeng Lu, Wei Shao, Edith Ngai, Xiping Hu, and Bin Hu. A new skeletal representation based on gait for depression detection. In *2020 IEEE International Conference on E-health Networking, Application Services (HEALTHCOM)*, pages 1–6, 2021.

[33] Yann LeCun, Yoshua Bengio, and Geoffrey Hinton. Deep learning. *nature*, 521(7553):436–444, 2015.

[34] Sebastien C Wong, Adam Gatt, Victor Stamatescu, and Mark D McDonnell. Understanding data augmentation for classification: when to warp? In *2016 international conference on digital image computing: techniques and applications (DICTA)*, pages 1–6. IEEE, 2016.

[35] Francisco J Moreno-Barea, Fiammetta Strazzera, José M Jerez, Daniel Urda, and Leonardo Franco. Forward noise adjustment scheme for data augmentation. In *2018 IEEE Symposium Series on Computational Intelligence (SSCI)*, pages 728–734. IEEE, 2018.

[36] Zhun Zhong, Liang Zheng, Guoliang Kang, Shaozi Li, and Yi Yang. Random erasing data augmentation. In *Proceedings of the AAAI Conference on Artificial Intelligence*, volume 34, pages 13001–13008, 2020.

[37] Diederik P Kingma and Max Welling. Auto-encoding variational bayes. *arXiv preprint arXiv:1312.6114*, 2013.

[38] Carl Doersch. Tutorial on variational autoencoders. *arXiv preprint arXiv:1606.05908*, 2016.

[39] Tero Karras, Samuli Laine, and Timo Aila. A style-based generator architecture for generative adversarial networks. In *Proceedings of the IEEE/CVF Conference on Computer Vision and Pattern Recognition*, pages 4401–4410, 2019.

[40] David Bau, Jun-Yan Zhu, Hendrik Strobelt, Bolei Zhou, Joshua B Tenenbaum, William T Freeman, and Antonio Torralba. Gan dissection: Visualizing and understanding generative adversarial networks. *arXiv preprint arXiv:1811.10597*, 2018.

[41] Jun-Yan Zhu, Taesung Park, Phillip Isola, and Alexei A Efros. Unpaired image-to-image translation using cycle-consistent adversarial networks. In *Proceedings of the IEEE international conference on computer vision*, pages 2223–2232, 2017.

[42] Kurt Kroenke, Robert L Spitzer, and Janet BW Williams. The phq-9: validity of a brief depression severity measure. *Journal of general internal medicine*, 16(9):606–613, 2001.

[43] William WK Zung. A self-rating depression scale. *Archives of general psychiatry*, 12(1):63–70, 1965.

[44] Microsoft kinect. https://msdn.microsoft.com. accessed on 11 January 2018.

[45] Tomasz Sapiński, Dorota Kamińska, Adam Pelikant, Cagri Ozcinar, Egils Avots, and Gholamreza Anbarjafari. Multimodal database of emotional speech, video and gestures. In *International Conference on Pattern Recognition*, pages 153–163. Springer, 2018.

[46] Pascal Gwosdek, Sven Grewenig, Andrés Bruhn, and Joachim Weickert. Theoretical foundations of gaussian convolution by extended box filtering. In *International Conference on Scale Space and Variational Methods in Computer Vision*, pages 447–458. Springer, 2011.

[47] Shiqi Yu, Daoliang Tan, and Tieniu Tan. A framework for evaluating the effect of view angle, clothing and carrying condition on gait recognition. In *18th International Conference on Pattern Recognition (ICPR'06)*, volume 4, pages 441–444. IEEE, 2006.

[48] Ralf Steuer, Jürgen Kurths, Carsten O Daub, Janko Weise, and Joachim Selbig. The mutual information: detecting and evaluating dependencies between variables. *Bioinformatics*, 18(suppl_2):S231–S240, 2002.

[49] Z. Hussain, F. Gimenez, D. Yi, and D. Rubin. Differential data augmentation techniques for medical imaging classification tasks. 2017.